Mon. Not. R. Astron. Soc. **000**, 000–000 (0000) Printed 4 March 2013 (MN LATEX style file v2.2)

High-energy emission from the pulsar striped wind: a synchrotron model for gamma-ray pulsars

Jérôme Pétri[1]
[1] *Observatoire Astronomique de Strasbourg, UMR 7550 Université de Strasbourg, CNRS, 11 rue de l'Université, 67000 Strasbourg, France*

Accepted . Received ; in original form 4 March 2013

ABSTRACT

Gamma-ray pulsars constitute a class of high and very high-energy emitters for which the known population is steadily increasing thanks to the Fermi/Large Area Telescope. Nowadays, more than a hundred such pulsars have been detected, offering a reasonable sample onto which to apply statistical techniques in order to outline relevant trends in the averaged properties of this (maybe not so) special class of pulsars. In this paper, their gamma-ray luminosity and spectral features are explained in the framework of synchrotron radiation from particles located in the stripe of the pulsar wind. Apart from radiative losses, particles are also subject to a constant re-acceleration and re-heating for instance by a magnetic reconnection induced electric field. The high-energy luminosity scales as $L_\gamma \approx 2\times 10^{26}\ \mathrm{W}\,(L_{\rm sd}/10^{28}\ \mathrm{W})^{1/2}\,(P/1\ \mathrm{s})^{-1/2}$ where $L_{\rm sd}$ is the pulsar spindown luminosity and P its period. From this relation, we derive important parameters of pulsar magnetosphere and wind theories. Indeed, we find bulk Lorentz factor of the wind scaling as $\Gamma_{\rm v} \approx 10\,\tau_{\rm rec}^{1/5}\,(L_{\rm sd}/10^{28}\ \mathrm{W})^{1/2}$, pair multiplicity κ related to the magnetization parameter σ by $\kappa\,\sigma\,\tau_{\rm rec}^{1/5} \approx 10^8$, and efficiency η of spin-down luminosity conversion into particle kinetic energy according to the relation $\eta\,\sigma \approx 1$. A good guess for the associated reconnection rate is then $\tau_{\rm rec} \approx 0.5\,(L_{\rm sd}/10^{28}\ \mathrm{W})^{-5/12}$. Finally, pulses in gamma-rays are visible only if $L_{\rm sd}/P \gtrsim 10^{27}$ W/s. This model differs from other high-energy emission mechanisms because it makes allowance not only for rotational kinetic energy release but also for an additional reservoir of energy anchored to the magnetic field of the stripe and released for instance by some magnetic reconnection processes.

Key words: Acceleration of particles - magnetic fields - radiation mechanisms: non-thermal - MHD - gamma-rays: theory - pulsars: general

1 INTRODUCTION

Since their discovery in the radio band more than 40 years ago, pulsars have now been firmly detected in all wavelengths of the electromagnetic spectrum, from radio through optical, X-ray and eventually high-energy gamma-rays. Recently the Crab was even detected in very-high energies by VERITAS (VERITAS Collaboration et al. 2011) and MAGIC (Aleksić et al. 2011). Although the radio emission mechanism remains poorly understood, the MeV-GeV pulsed emission puts severe constraints on the high-energy counterpart radiation models. The new catalog of gamma-ray pulsars obtained by the Fermi-LAT instrument (Abdo et al. 2010) increased the number of gamma-ray pulsars from seven to about fifty. Since then, new pulsars are discovered regularly, more than hundred are listed nowadays (Nolan et al. 2012). This allows for the first time a reasonable statistical analysis of the high-energy emission properties of these objects like spectral shapes, cut-off energies, and comparison between radio and gamma-ray radiation if both are available.

It was long suspected that polar cap or outer/slot gaps could explain this emission. Nevertheless, recent Fermi observations clearly disfavored the polar cap explanation (Abdo et al. 2010). Some of these gamma-ray pulsars do not significantly show a spectral cut-off around a few GeV but rather a significant change in the spectral index of the power law. Moreover MAGIC/VERITAS detection of the Crab above 100 GeV seems to rule out outer gap models because the accelerating electric field combined to radiation reaction limited flow renders it difficult to observe photons above a few GeV. The determination of the precise location of the emission regions is still problematic. The in phase pulsation observed in both gamma-ray and in radio for some millisecond pulsars (Guillemot et al. 2012) furnishes one more apparent contradiction between radio and high-energy emission mechanisms. Do they eventually originate

in the same place in the magnetosphere or in the wind? But why are then some gamma-ray pulsars radio quiet as those seen by Pletsch et al. (2012). We are still far from a consensus on the emission model, be it in the radio band or in gamma-rays.

Radio pulses and gamma-ray photons are expected to be produced in different emission sites, probably close to the neutron star surface for the former, described by a polar cap model (Radhakrishnan & Cooke 1969), and in the vicinity of the light-cylinder for the latter, explained by outer gaps (Cheng et al. 1986).

Recently, gamma-ray light-curves have been computed for a realistic magnetospheric model based on 3D MHD simulations of the near pulsar magnetosphere (Bai & Spitkovsky 2010). In this model, gamma rays are expected close to the light-cylinder.

An alternative site for the production of pulsed radiation has been investigated a few years ago by Kirk et al. (2002). This model is based on the striped pulsar wind, originally introduced by Coroniti (1990). Emission from the striped wind originates outside the light cylinder and relativistic beaming effects are responsible for the phase coherence of this radiation (Pétri 2009, 2011)

In this paper, we show that the pulsed high-energy emission up to a few GeV as observed by Fermi/LAT can be explained by synchrotron radiation emanating from the relativistically hot current sheet present in the pulsar striped wind. Our approach follows the study done by Lyubarskii (1996) who included possible pair creation which are discarded in the present work. Sec. 2 describes the dynamics and geometry of the relativistic plasma flow as well as the radiation model. Then Sec. 3 derives some important constraints on the bulk Lorentz factor of the wind, the pair multiplicity factor, the magnetization parameter as well as a criterion for gamma-ray pulsar detection. Conclusions are drawn in Sec. 4.

2 THE SYNCHROTRON STRIPED WIND MODEL

Synchrotron emission from the striped wind applies successfully to the pulsed optical polarization properties of the Crab pulsar (Pétri & Kirk 2005). Our aim is to extend to the highest possible energies the synchro-photons emanating from the current sheet. In the present work, we are not concerned with the phase-resolved emission nor in the polarization properties, but we only focus on the average gamma-ray features of the Fermi/LAT detected pulsars depending on two fundamental observables: the period P of the pulsar and its first derivative $\dot{P}$. We emphasize that this two-parameter family of model remains very restrictive and will not be able to explain in detail each individual pulsar. Indeed, the mechanisms occurring in the current sheet are far from being understood, as they involve micro-physics that has not yet been addressed self-consistently and linked to the overall structure and dynamics of the magnetosphere and wind. Nevertheless, as we will show, our model is able to reproduce qualitatively and quantitatively the full set of Fermi data with reasonable accuracy. The derived parameters such as wind Lorentz factor, pair multiplicity and magnetization are consistent with values obtained from other independent considerations, giving us confidence in our description of the emission mechanism.

2.1 Plasma configuration

At the heart of any pulsar emission model, be it radio, optical or X-rays/gamma-rays, there is a (possibly relativistic) plasma flowing in a strongly magnetized field, preferentially within the magnetosphere for the polar cap and slot/outer gaps. Contrary to these models, we assume that the pulsed emission is produced within the current sheet of the striped wind, thus well outside the magnetosphere, a place where the magnetic configuration switches from poloidal dominant to toroidal dominant. The plasma in this current sheet is the crucial ingredient in our model. It is embedded in a mostly non emitting cold plasma. More precisely, the striped wind flow is made of two distinct parts, namely

- a cold and strongly magnetized plasma of particle density number $n_{\rm c}$ and Lorentz factor $\Gamma_{\rm v}$, as measured in the lab frame. Note that $\Gamma_{\rm v}$ corresponds to the bulk Lorentz factor of the whole striped wind structure. This part of the wind does not radiate significantly.
- a hot and tenuous but weakly magnetized plasma of particle density number $n_{\rm h}$ occupying a fraction Δ of the wavelength of the wind $\lambda_{\rm v} = 2\,\pi\,\beta_{\rm v}\,r_{\rm L}$, also measured in the lab frame. The fraction of hot plasma is negligible with respect to the cold part, i.e. $\Delta \ll 1$. $r_{\rm L} = c/\Omega$ is the light-cylinder radius, $\beta_{\rm v} = v/c$ the wind speed normalized to the speed of light c and Ω the stellar rotation rate.

Later on, it will be useful to deal with the proper densities and proper lengths given by $n_{\rm c} = \Gamma_{\rm v}\,n'_{\rm c}$, $n_{\rm h} = \Gamma_{\rm v}\,n'_{\rm h}$ and $\lambda'_{\rm v} = \Gamma_{\rm v}\,\lambda_{\rm v}$. Proper quantities in the rest frame of the wind are always primed except for thermodynamical quantities such as pressure and temperature which are meaningful only in the proper frame. Furthermore, we assume that pairs are created within the magnetosphere and cool down quickly before reaching the wind zone. Therefore, they exclusively replenish the cold part of the striped wind. Acceleration and heating of particles occurs once in the stripe and not before. This is clearly an additional source of energy, a kind of magnetic luminosity, independent of the spin-down luminosity of the pulsar. Therefore, rotational kinetic energy is spent to produce relativistic leptons with a curvature radiation reaction limited Lorentz factor of about $\gamma \approx 10^7$. They will cool down in the magnetized part of the wind because of magnetic field strength around the light-cylinder higher than 10^{-2} T according to Fermi/LAT first pulsar catalog (Abdo et al. 2010). Indeed, the synchrotron cooling time $\tau_{\rm syn} \approx 7.7\,{\rm s}\,\gamma^{-1}\left(\frac{B}{1\,{\rm T}}\right)^{-2}$ is much less than the period of a pulsar. In the most unfavored case, radiation losses are still such that $\tau_{\rm syn} \lesssim 1$ ms. Thus, our model can apply irrespective of the period of the pulsar, millisecond or normal.

2.2 Wind flow

Although the hot plasma is much less populated than the cool part, it radiates significantly more because of its relativistic temperature. Indeed, to ensure a quasi-stationary equilibrium state, magnetic pressure outside the stripe has to be compensated by gaseous pressure inside the current

sheet. Thus in the wind frame, pressure balance implies

$$\frac{1}{3}\,\gamma'_{\rm h}\,n'_{\rm h}\,m_{\rm e}\,c^2 = \frac{B'^2}{2\,\mu_0} \tag{1}$$

$m_{\rm e}$ is the electron rest mass and μ_0 vacuum permeability. We recall that the magnetic field is essentially toroidal in the wind zone, a Lorentz boost thus gives $B' = B/\Gamma_{\rm v}$ where $B = B_L\,r_{\rm L}/r$, B_L being the magnetic field strength at the light-cylinder. The Lorentz factor $\gamma'_{\rm h}$ can be deduced from considerations about the dynamics in the current sheet as explained in the next paragraph (see Eq.(6)), leading to the knowledge of the density of the hot plasma $n'_{\rm h}$ as given by the pressure balance Eq. (1).

The bulk kinetic energy of the wind is extracted from the spin-down luminosity of the pulsar. Noting η the efficiency coefficient of rotational to particle energy conversion, the plasma kinetic energy density is

$$\Gamma_{\rm v}\,n_{\rm c}\,m_{\rm e}\,c^2 = \eta\,\frac{L_{\rm sd}}{4\,\pi\,r^2\,c} \tag{2}$$

Note that we neglect the contribution of the hot component because $\Delta \ll 1$ and $L_{\rm sd} = 4\,\pi^2\,I\,\dot{P}\,P^{-3}$ is the spin-down luminosity and $I = 10^{38}$ kg m^2 the neutron star moment of inertia. Moreover, the cold plasma density is related to the pair creation rate $\dot{N}_\pm$ (particles generated per second) by $4\,\pi\,r^2\,c\,n_{\rm c} = \dot{N}_\pm$ where the contribution from both poles are taken into account and

$$\dot{N}_\pm \approx 2.77\times10^{30}\ {\rm s}^{-1}\,\kappa\,\left(\frac{P}{1\ s}\right)^{-2}\,\left(\frac{B_{\rm ns}}{10^8\ {\rm T}}\right)\,\left(\frac{R_{\rm ns}}{10\ {\rm km}}\right)^3 \tag{3}$$

κ is the usual pair multiplicity factor, e the absolute value of the charge of an electron, ε_0 the vacuum permittivity, $B_{\rm ns}$ the stellar surface magnetic field intensity and $R_{\rm ns}$ the neutron star radius. Inserting Eq. (3) into Eq. (2), we found a relation between $\Gamma_{\rm v}, \kappa$ and η such that

$$\Gamma_{\rm v}\,\kappa \approx 8.7\times10^8\,\eta\,\left(\frac{L_{\rm sd}}{10^{28}\ {\rm W}}\right)^{1/2} \tag{4}$$

A similar relation holds for the magnetization defined by $\sigma = B^2/(\mu_0\,\Gamma_{\rm v}\,n_{\rm c}\,m_{\rm e}\,c^2)$. The magnetization parameter is approximately the inverse of the efficiency coefficient, i.e.

$$(1+\sin^2\chi)\,\sigma\,\eta = 1 \tag{5}$$

where χ is the pulsar obliquity and assuming the force-free spin-down luminosity of Spitkovsky (2006) and confirmed by Pétri (2012). This reduces the number of independent parameters in the model. As expected, the fraction of spin-down luminosity converted into particles remains weak $\eta \ll 1$ as long as the magnetization parameter remains large $\sigma \gg 1$.

2.3 Dynamics in the current sheet

It is usually claimed that the total gamma-ray luminosity should not exceed the spin-down luminosity. Actually, this assertion only holds if the rotation of the neutron star is the unique source of energy. Another non negligible reservoir could be the magnetic field itself. We will indeed assume that part of the radiation is due to magnetic reconnection within the current sheet. This will alleviate the restriction $L_\gamma \leq L_{\rm sd}$ although the model not necessarily violates this condition. It will be checked a posteriori.

Particles in the sheet lose energy due to synchrotron cooling. However, a stationary state in the wind frame can be reached if particles re-energize by acceleration in a reconnecting magnetic field configuration. The key parameter is the collisionless reconnection rate, $\tau_{\rm rec}$. It will be constrained from spectral features of the Fermi/LAT data. This means that the induced electric field re-accelerating particles is of the order $E_{\rm rec} \approx \tau_{\rm rec}\,c\,B$. Equaling the synchrotron cooling timescale with the acceleration timescale in the reconnection layer, we find that the maximum Lorentz factor of the leptons (we use primed quantity to express the fact that they are evaluated in the wind frame) is

$$\gamma'_{\rm h} = \sqrt{\frac{3}{2}\,\frac{\mu_0\,e\,c}{\sigma_T\,B'_L}\,\frac{r}{r_{\rm L}}\,\tau_{\rm rec}} \tag{6}$$

Basically, it depends on the magnetic field strength at the light cylinder and on the distance to the centre of the pulsar. For these Lorentz factors, the typical energy of a synchrotron photons as seen in the wind frame is

$$\varepsilon'_B = \frac{3}{2}\,\gamma'^2_{\rm h}\,\frac{B'}{B_q}\,m_{\rm e}\,c^2 = \frac{9}{4}\,\frac{\mu_0\,e\,m_{\rm e}\,c^3}{\sigma_T\,B_q}\,\tau_{\rm rec} \tag{7}$$

where $B_q \approx 4.4\times10^9$ T is the quantum magnetic field. Thus the synchro-photon energy does only depend linearly on the reconnection rate. Interestingly the photon lies in the MeV band because $\varepsilon'_B = 236$ MeV $\tau_{\rm rec}$. Back to the lab frame, the photon is boosted by a Lorentz factor at most $2\,\Gamma_{\rm v}$ thus

$$\varepsilon_B = 2\,\Gamma_{\rm v}\,\varepsilon'_B = 472\ {\rm MeV}\,\Gamma_{\rm v}\,\tau_{\rm rec}. \tag{8}$$

According to the Fermi/LAT catalog (Abdo et al. 2010), the cut-off energy lies in the range 0.2-8 GeV. In our model, we interpret this cut-off more properly as a break in the spectral energy distribution. To make the idea more precise, think about an inverse Compton spectrum evolving from the Thomson regime to the Klein-Nishina regime. There is a break in the power law entailing precious information on the underlying emitting plasma. Here, the break is a consequence of the rapid cooling of electrons more energetic than $\gamma'_{\rm h}\,m_{\rm e}\,c^2$. Using a fiducial value of $\tau_{\rm rec} \approx 0.1$, we see that the Lorentz factor of the wind should be around $\Gamma_{\rm v} \in [5, 10^2]$. We emphasize that the estimates given here should be understood as orders of magnitude roughly within a factor 10. More confidently we expect $\Gamma_{\rm v} \in [1, 10^3]$ as will be shown from the observations. Moreover, the reliability of the value of the cut-off energy is probably doubtful at least for the most energetic pulsars like the Crab if not for almost the whole sample of gamma-ray pulsars.

2.4 Synchrotron luminosity

In the frame of the current sheet, relativistic particles in the hot component radiate synchrotron power at a rate $P'_{\rm syn}(\gamma'_{\rm h}, B') = (4/3)\,\sigma_T\,c\,\gamma'^2_{\rm h}\,U'_B$ where $U'_B = B'^2/(2\,\mu_0)$ is the magnetic energy density in the wind frame. The total emissivity of the hot plasma, assuming isotropy is $j'_{\rm syn}(\nu') = (n'_{\rm h}/(4\,\pi))\,P'_{\rm syn}(\gamma'_{\rm h}, B')\,\delta(\nu' - \nu'_{\rm syn})$ where $\nu'_{\rm syn} = (3/2)\,\gamma'^2_{\rm h}\,e\,B'/m_{\rm e}$. By Lorentz transformation and using relativistic invariants, the total synchrotron luminosity, boosted to the observer frame (expected to be interpreted as the

gamma-ray luminosity) is

$$L_{\rm syn} = 8.7\times10^{-20}\ {\rm W}\sqrt{\frac{\tau_{\rm rec}}{\alpha}}\,\frac{\Delta}{\Gamma_{\rm v}^{5/2}}\,L_{\rm sd}^{5/4}\sqrt{\frac{L_{\rm sd}}{P}} \qquad (9)$$

where $\Gamma_{\rm v}\geq1$ is the bulk Lorentz factor of the wind, $\Delta\leq1$ the thickness of the current sheet in fraction of the wavelength $\lambda_{\rm v}$, and $\alpha\geq1$ sets the minimum distance where emission starts (in the region $r\geq\alpha\,r_{\rm L}$). From eq. (4), we get

$$L_{\rm syn} = 3.9\times10^{-7}\ {\rm W}\sqrt{\frac{\tau_{\rm rec}}{\alpha}}\left(\frac{\kappa}{\eta}\right)^{5/2}\Delta\sqrt{\frac{L_{\rm sd}}{P}} \qquad (10)$$

Knowing the synchrotron luminosity Eq. (10) and the relations (4) and (5), we are able to deduce important constraints on the fundamental parameters. Theoretically, for fixed $\{\alpha,\Delta,\kappa,\eta,\tau_{\rm rec}\}$, our model predicts $L_{\rm syn}\propto\sqrt{L_{\rm sd}/P}$.

3 RESULTS

In this paragraph, we discuss the implication of the striped synchrotron model and the latest Fermi/LAT detections and give explicit values for the most relevant parameters of pulsar magnetosphere and wind theories.

3.1 Luminosity and spectral features

It is possible to relate $\Gamma_{\rm v}$ to the pair multiplicity κ and to the magnetization σ. According to the second source catalog (2FGL) (Nolan et al. 2012), a good fit of the whole sample of gamma-ray pulsars following the formal dependence as suggested by Eq. (10) thus with respect to $\sqrt{L_{\rm sd}/P}$ is

$$L_\gamma\approx2\times10^{26}\ {\rm W}\left(\frac{L_{\rm sd}}{10^{28}\ {\rm W}}\right)^{1/2}\left(\frac{P}{1\ {\rm s}}\right)^{-1/2} \qquad (11)$$

The constant of proportionality comes from Fermi/LAT data and will be compared to the factor in front of $\sqrt{L_{\rm sd}/P}$ in Eq. (10). Note that the integral energy flux above 100 MeV from 2FGL and distances from ATNF are subject to several sources of uncertainties (Manchester et al. 2005)[1]. This reflects into the derived quantities such as $\{\Gamma_{\rm v},\tau_{\rm rec},\Delta,\alpha\}$ for which the same remarks hold. We also used a beaming factor of 1. Thanks to the above fit, Eq. (11), and to the relation (10), we get $(\kappa/\eta)^{5/2}\,\Delta\,\sqrt{\tau_{\rm rec}/\alpha}\approx5\times10^{18}$. Adopting typical values of $\Delta\approx0.1$, $\alpha\approx10$, the relation between pair multiplicity and efficiency becomes $\kappa\,\tau_{\rm rec}^{1/5}\approx1.2\times10^8\,\eta$. From this, we immediately deduce the bulk Lorentz factor of the wind

$$\Gamma_{\rm v}\approx10\,\tau_{\rm rec}^{1/5}\left(\frac{L_{\rm sd}}{10^{28}\ {\rm W}}\right)^{1/2} \qquad (12)$$

It is proportional to the square root of the spin-down luminosity. By comparison between the cut-off energies observed by Fermi/LAT and the prediction Eq. (8), we can constrain the reconnection rate for each pulsar such that

$$\tau_{\rm rec}\approx\left(\frac{4.72\ {\rm GeV}}{E_{\rm cut}({\rm GeV})}\right)^{-5/6}\left(\frac{L_{\rm sd}}{10^{28}\ {\rm W}}\right)^{-5/12} \qquad (13)$$

[1] see also the website from ATNF
http://www.atnf.csiro.au/research/pulsar/psrcat/expert.html

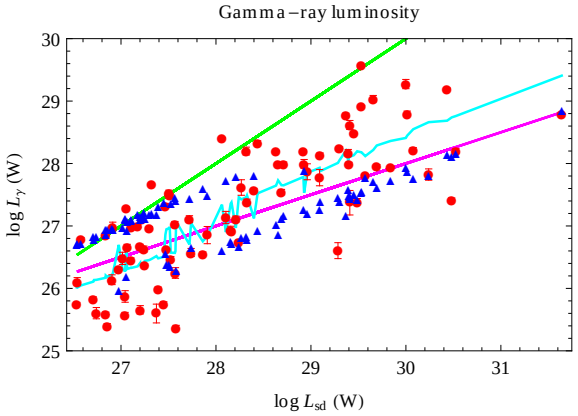

Figure 1. Pulsar gamma-ray luminosity L_γ versus spin-down luminosity $L_{\rm sd}$. Fermi observations are depicted by red points whereas the predicted luminosity is presented by blue triangles. The magenta line corresponds to the law $L_\gamma=10^{26}\ {\rm W}\,(L_{\rm sd}/10^{26}\ {\rm W})^{1/2}$, the green line to $L_\gamma=L_{\rm sd}$ and the cyan line to the best fit Eq. (11).

The reconnection rate is about unity for low $L_{\rm sd}$ pulsars such as the millisecond ones. This might be possible if the background pair density is about 1% of the current sheet particle density number (Bessho & Bhattacharjee 2012). We suspect magnetic dissipation to reach its maximal possible value for those pulsars with $L_{\rm sd}\leq10^{28}$ W whereas $\tau_{\rm rec}$ decreases monotonically down to 0.01 for the brightest pulsars with $L_{\rm sd}\geq10^{28}$ W. This splits the gamma-ray pulsars population into two groups, a first with reconnection pushed to its highest limit and a second with less drastic reconnection rate. Moreover, the photon spectral indexes founded by Fermi/LAT fall in the range $\Gamma\in[0.6,2]$. This is consistent with a synchrotron spectrum emanating from a power law distribution of leptons with $p\in[1,3]$ and $dn_{\rm h}/d\gamma(\gamma)\propto\gamma^{-p}$. This could be explained by a relativistic kinetic reconnection process, either very localized close to the X-point where it is found that $p\approx1$, or on a global scale, within an extended region such as a simulation box for PIC simulations (Jaroschek et al. 2004) where $p\approx3$. A detailed analysis of the kinetic reconnection processes is out of the scope of this letter but see Zenitani & Hoshino (2007). Detailed knowledge of the particle distribution functions within the current sheet awaits extensive PIC simulations with radiation effects included (Jaroschek & Hoshino 2009). The results of our model concerning the expectation about the gamma-ray luminosity are summarized in the plot Fig. 1. We show the gamma-ray luminosity versus the spin-down luminosity for a large sample of gamma-ray pulsars. The predicted luminosity, blue triangles, is overlapped to the Fermi/LAT data, red points. Although not explicitly imposed by our model and actually not required, the gamma-ray luminosity nevertheless satisfies $L_\gamma\lesssim L_{\rm sd}$.

3.2 Condition for pulsed gamma-ray emission

Gamma-ray emitters are identified as pulsars because of their very stable clock. In our model, pulsation is a consequence of the combination of relativistic beaming and striped wind structure. Therefore, we expect to observe MeV-GeV pulsed emission only if the stripe survives the de-

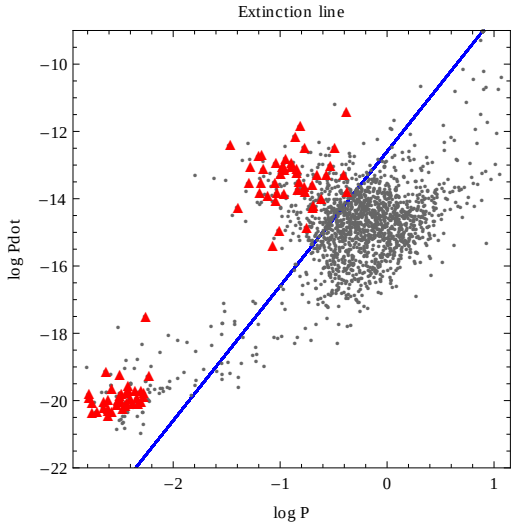

Figure 2. The extinction line for gamma-ray pulsation in the $P\dot{P}$ diagram. All radio pulsars are shown in grey points whereas Fermi/LAT detected gamma-ray pulsars are in red triangles. They all satisfy our criterion Eq. (14), lying above the blue extinction line.

structive influence of magnetic dissipation due to reconnection. Assuming as a first approximation that the stripe resembles a relativistic Harris current sheet, a stationary equilibrium can exist only if the drift speed of the leptons within the sheet is less than the speed of light. This is actually a criterion for reconnection as explained in Kirk & Skjæraasen (2003). In the wind frame, the drift speed is given by $\beta'_{\rm d} = r'_B/(\Delta\,\lambda'_{\rm v})$ where r'_B is the proper Larmor radius. Replacing the bulk Lorentz factor of the wind by the approximate relation Eq. (12), we derive a simple criterion for pulsed emission from the condition $\beta'_{\rm d} \leq 1$. According to its spin-down luminosity and to its period, a pulsar will be detected as gamma-ray emitter if $L_{\rm sd}/P \gtrsim (10^{23}\ {\rm W/s})\,\tau_{\rm rec}\,\alpha^3/\Delta^2$. For typical pulsar parameters, we found

$$\frac{L_{\rm sd}}{P} \gtrsim 10^{27}\ {\rm W/s} \qquad (14)$$

This criterion is shown in Fig. 2 for the Fermi/LAT pulsar second catalog and marked as a blue line. All detected pulsars fall into this criterion. The two populations of pulsars, millisecond and normal, are clearly distinguishable. The gap between the extinction line and the detected millisecond pulsar is due to the P^{-1} law in Eq. (14). The average parameters $(\alpha, \Delta, \tau_{\rm rec})$ may also be slightly different of those from normal pulsars. The absence of pulsation does not imply that the underlying neutron star is not a gamma-ray emitter, it just says that it will not be seen as a gamma-ray pulsar.

4 CONCLUSION

In this paper, we showed that the pulsed MeV-GeV emission from gamma-ray pulsars can be explained by a synchrotron model in the striped pulsar wind including some magnetic reconnection. Relevant average parameters of our model are given by $\Delta \approx 0.1$ and $\alpha \approx 10$. The reconnection rate $\tau_{\rm rec}$ and bulk Lorentz factor of the wind $\Gamma_{\rm v}$ are explicit functions of $L_{\rm sd}$. Moreover the predicted extinction line is in agreement with gamma-ray pulsar observations.

Our synchrotron model predicts a clear break in the spectra around a few GeV depending on the bulk Lorentz factor and reconnection rate. In order to explain recent observations by VERITAS and MAGIC, this picture should be supplemented with an inverse Compton counterpart. The model would also benefit from phase-resolved high-energy polarization measurements which are highly discriminating for current models.

ACKNOWLEDGMENTS

I am grateful to David A. Smith for stimulating discussions and careful reading of the manuscript.

REFERENCES

Abdo, A. A., Ackermann, M., Ajello, M., et al. 2010, ApJS, 187, 460
Aleksić, J., Alvarez, E. A., Antonelli, L. A., et al. 2011, ApJ, 742, 43
Bai, X. & Spitkovsky, A. 2010, ApJ, 715, 1282
Bessho, N. & Bhattacharjee, A. 2012, ApJ, 750, 129
Cheng, K. S., Ho, C., & Ruderman, M. 1986, ApJ, 300, 500
Coroniti, F. V. 1990, ApJ, 349, 538
Guillemot, L., Johnson, T. J., Venter, C., et al. 2012, ApJ, 744, 33
Jaroschek, C. H. & Hoshino, M. 2009, Physical Review Letters, 103, 075002
Jaroschek, C. H., Lesch, H., & Treumann, R. A. 2004, ApJL, 605, L9
Kirk, J. G. & Skjæraasen, O. 2003, ApJ, 591, 366
Kirk, J. G., Skjæraasen, O., & Gallant, Y. A. 2002, A&A, 388, L29
Lyubarskii, Y. E. 1996, A&A, 311, 172
Manchester, R. N., Hobbs, G. B., Teoh, A., & Hobbs, M. 2005, Astr. J., 129, 1993
Nolan, P. L., Abdo, A. A., Ackermann, M., et al. 2012, ApJS, 199, 31
Pétri, J. 2009, A&A, 503, 13
Pétri, J. 2011, MNRAS, 412, 1870
Pétri, J. 2012, ArXiv e-prints
Pétri, J. & Kirk, J. G. 2005, ApJL, 627, L37
Pletsch, H. J., Guillemot, L., Allen, B., et al. 2012, ApJ, 744, 105
Radhakrishnan, V. & Cooke, D. J. 1969, Astrophysical Letters, 3, 225
Spitkovsky, A. 2006, ApJL, 648, L51
VERITAS Collaboration, Aliu, E., Arlen, T., et al. 2011, Science, 334, 69
Zenitani, S. & Hoshino, M. 2007, ApJ, 670, 702